

# Identification of the Binding Site for a Low-Molecular-Weight Inhibitor of Plasminogen Activator Inhibitor Type 1 by Site-Directed Mutagenesis

Petter Björquist,<sup>‡</sup> Johanna Ehneborg,<sup>‡</sup> Tord Inghardt,<sup>§</sup> Lennart Hansson,<sup>||</sup> Maria Lindberg,<sup>||</sup> Marcel Linschoten,<sup>§</sup> Mats Strömquist,<sup>||</sup> and Johanna Deinum<sup>\*,‡</sup>

Biochemistry and Medicinal Chemistry, Preclinical R&D, Astra Hässle AB, S-431 83 Mölndal, and Molecular Biology, Preclinical R&D, Astra Hässle AB, Tvistevägen 48, S-901 87 Umeå, Sweden

Received June 27, 1997; Revised Manuscript Received November 5, 1997

**ABSTRACT:** A novel low-molecular-weight inhibitor, AR-H029953XX, was developed from a known fibrinolytic compound, flufenamic acid, which prevented complex formation of human plasminogen activator inhibitor type 1 (PAI-1) with tissue plasminogen activator (tPA) by inhibition of PAI-1. To explore the binding site for AR-H029953XX, mutants of human PAI-1 were constructed by site-directed mutagenesis and were then expressed in CHO cells, purified, activated, and characterized. (1) PAI-1 with mutations in the reactive center loop: L1-PAI-1 (P10, Ser337Glu) had stability and activity similar to those of wild-type PAI-1 (wt-PAI-1), and L2-PAI-1 (P12, Ala335Glu) was highly stable but was a substrate for tPA. (2) PAI-1 with mutations near the binding epitope for the strongly inhibiting monoclonal antibody CLB-2C8: C1-PAI-1 (Phe114Glu), C2-PAI-1 (Val121Phe), C3-PAI-1 (Arg76Glu/Arg115Glu/Arg118Glu), and C4-PAI-1 (Arg115Glu) were all comparable in activity and stability to wt-PAI-1. AR-H029953XX ( $K_i = 25 \mu\text{M}$ ) prevented complex formation between tPA and active wt-PAI-1 as well as that with mutants L1-, L2-, C1-, C2-, and C4-PAI-1. AR-H029953XX also inhibited binding of these PAI-1 variants to the antibody CLB-2C8, as measured by surface plasmon resonance. In contrast, AR-H029953XX had almost no inhibitory effect on the complex formation of tPA with C3-PAI-1. Moreover, AR-H029953XX had no effect on the binding rate of CLB-2C8 to C3-PAI-1, or on the binding to latent PAI-1 or to cleaved L2-PAI-1. The binding site of AR-H029953XX thus appears to be located in the neighborhood of the postulated epitope for CLB-2C8, near residues Arg76 and/or Arg118. This specific domain of the PAI-1 molecule might thus also be important for the mechanism of inhibitory activity toward tPA. Moreover, the structure of this region in active PAI-1 has to be different from the corresponding regions in latent and cleaved PAI-1.

The serpin PAI-1<sup>1</sup> binds irreversibly to tPA and totally inhibits tPA activity (1). PAI-1 is the main physiological inhibitor of tPA in plasma and may play a role in the development of thromboembolic diseases (2). Thus, specific inhibition of plasma PAI-1 activity might provide a novel and therapeutically valuable means of enhancing fibrinolysis in humans. In animal models, PAI-1-inhibiting antibodies have been shown to enhance fibrinolysis significantly (3, 4). A low-molecular-weight compound, XR5118, has also recently been reported to enhance fibrinolysis via inhibition of PAI-1 (5). Finally, peptides corresponding to portions of the PAI-1 reactive center loop did slowly inhibit PAI-1 activity in vitro (6, 7). However, no conclusive information concerning the mechanism of PAI-1 inhibition by these different compounds has been published so far.

We have searched for general information regarding the three-dimensional structure of active PAI-1 and, in particular, possible binding sites for small, synthetic inhibitors. In this report, we present data on a new class of PAI-1 inhibitors. The anthranilic acid derivative AR-H029953XX (Figure 1) was developed from the known fibrinolysis enhancer flufenamic acid (8), which we found inhibits PAI-1. In the search for possible interaction sites for low-molecular-weight inhibitors for PAI-1, not only the residues in the reactive center loop but also the binding epitopes for different inhibiting antibodies are of interest. Thus, to provide structural information pertaining to the rational design and optimization of these compounds, we have constructed and characterized mutants of PAI-1. For the design of these mutants, we have therefore created a model of active PAI-1 (Figure 2A) based on the coordinates of the structurally closely related serpin antithrombin III (9), since the structures of only latent (10) and cleaved (11) PAI-1 are known.

PAI-1 is an unusual serpin since the active conformation spontaneously rearranges into the latent, inactive form (1) which no longer can bind irreversibly to tPA. In latent PAI-1, 13 residues of the reactive center loop (P16–P4) are inserted into  $\beta$ -sheet A as strand 4A. Prevention of this loop insertion appears to transform active PAI-1 into a tPA-substrate which is rapidly cleaved at P1–P1' followed by dissociation of the

\* To whom correspondence should be addressed: Biochemistry, Preclinical R&D, Astra Hässle AB, S-431 83 Mölndal, Sweden. Telephone: +46 31 7761592. Fax: +46 31 7763736. E-mail: Johanna.Deinum@hassle.se.astra.com.

<sup>‡</sup> Biochemistry, Astra Hässle, Mölndal.

<sup>§</sup> Medicinal Chemistry, Astra Hässle, Mölndal.

<sup>||</sup> Molecular Biology, Astra Hässle, Umeå.

<sup>1</sup> Abbreviations: CHO, Chinese hamster ovary; HEPES, 4-(2-hydroxyethyl)-1-piperazineethanesulfonic acid; PAI-1, plasminogen activator inhibitor type-1; wt, wild-type; RAM Fc, rabbit anti-mouse fragment crystalline; RU, resonance units; serpin, serine proteinase inhibitor; tPA, two-chain tissue plasminogen activator.

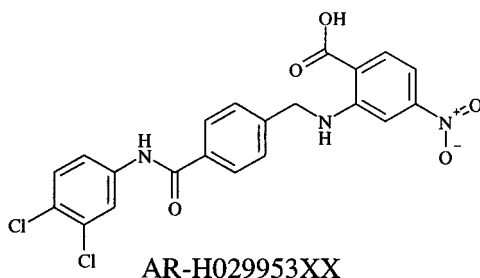


FIGURE 1: Structure of the low-molecular-weight PAI-1 inhibitor AR-H029953XX.

complex (12–14). Two loop mutants, L1-PAI-1 (P10, Ser337Glu) and L2-PAI-1 (P12, Ala335Glu) (see Figure 2), were constructed to investigate whether AR-H029953XX interacts with loop insertion. We furthermore predicted that prevention of loop insertion using site-directed mutagenesis might provide a stable, functional form of PAI-1 more amenable to crystallization. A randomly mutated PAI-1 library containing clones with improved half-lives has been published (15), but these mutants are still not sufficiently stable for the purpose of crystallization.

Of the three different binding domains for inhibiting antibodies that have been recognized (16), only the binding epitope for CLB-2C8 has been more precisely defined. The epitope for CLB-2C8 is located in a domain spanning amino acids 110–145 (17), later restricted to residues 128–145 (18). We therefore examined the surface of PAI-1 within and in the vicinity of this epitope for potential binding sites for AR-H029953XX (see Figures 2 and 3), and since we have found that the acidic function of AR-H029953XX is essential for inhibitory activity, we were particularly interested in finding positively charged domains. The most likely site for binding of this low-molecular-weight inhibitor appeared to be a hydrophobic cleft near residues Phe114 and Val121, flanked by a basic surface region containing three arginine residues (76, 115, and 118). Four different PAI-1 mutants with alterations in this area, C1–4-PAI-1 (Figure 2B), were constructed, and the possibility of AR-H029953XX interfering with the binding of these mutants to tPA and to CLB-2C8 was studied.

We here propose that this new domain near the CLB-2C8 binding epitope of PAI-1 constitutes the binding site for the low-molecular-weight inhibitor AR-H029953XX.

## MATERIALS AND METHODS

**Chemicals.** Tween 80 was purchased from Sigma Chemical Co. (St. Louis, MO), and a solution of surfactant P 20 (10% Tween 20) was obtained from BIAcore AB (Uppsala, Sweden). Flavigen tPA ( $\text{CH}_3\text{SO}_2\text{-D-HHT-Gly-Arg-pNA}$ ) was obtained from Biopool (Umeå, Sweden). AR-H029953XX (see Figure 1) and its corresponding tetrazolo-amidino and nitro derivatives were synthesized at Astra Hässle AB (Mölnådal, Sweden). Flufenamic acid [*N*-[3-(trifluoromethyl)phenyl]anthranilic acid] was obtained from Aldrich-Chemie GmbH and Co. (Steinheim, Germany). The low-molecular-weight inhibitors were first dissolved in DMSO and then diluted to 1% DMSO with assay buffer.

**Proteins.** The mouse anti-human PAI-1 monoclonal IgG<sub>1</sub> antibody CLB-2C8 was obtained from the Dutch Red Cross (Amsterdam, The Netherlands). A solution of rabbit anti-



FIGURE 2: Model of active PAI-1 constructed from the coordinates of antithrombin III (9). (A, top) The position of side chains of the cleavage site (P1–P1') and the mutated amino acids in the reactive center loop are highlighted: L1-PAI-1 (P10), Ser337Glu; and L2-PAI-1 (P12), Ala335Glu. The binding epitope for CLB-2C8, residues 110–145 (17), is shown in red. (B, bottom) Side view showing details of the CLB-2C8 epitope with the mutated amino acids in mutants C1–4-PAI-1 highlighted (see the text for details of the mutations).

mouse Fc (RAM Fc) was purchased from BIAcore AB. The mouse anti-human tPA monoclonal IgG<sub>1</sub> antibody 2:2 B10 was obtained from IMCO Corporation Ltd. (Stockholm, Sweden). Wild-type human PAI-1 from CHO cells was purified and activated as described before (19). Two-chain tPA from human melanoma cells was obtained from Biopool (Umeå, Sweden). The molar protein concentrations of the ultracentrifuged protein solutions of PAI-1 and tPA were

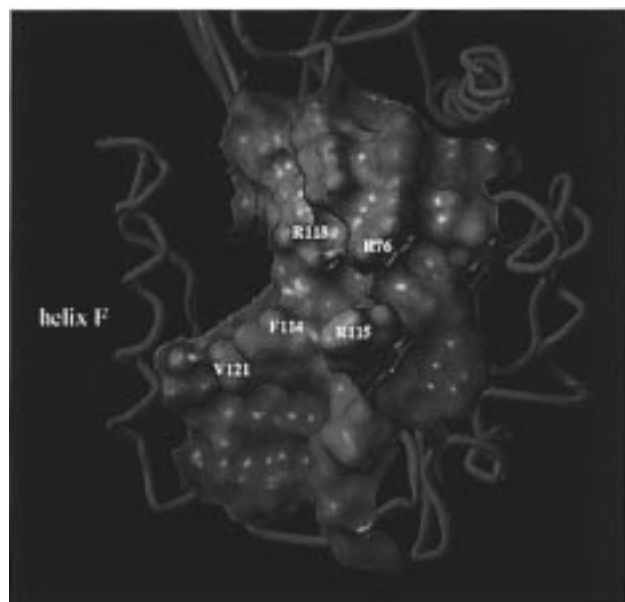


FIGURE 3: Electrostatic potential distribution map of the hypothesized binding domain, centered around residue 115, modeled from the coordinates of latent PAI-1 (10) positioned as in Figure 2B. Red depicts positive potential, blue negative potential, and green neutral or hydrophobic areas. The positions of the mutated residues are indicated.

determined using the recently found  $\epsilon_{280}$  (20). The proteins were stored and handled as previously described (16).

**Buffers.** Buffer A consisted of 50 mM Tris, 100 mM NaCl, and 0.1 g/L Tween 80 and buffer B of 10 mM HEPES, 150 mM NaCl, 3.4 mM EDTA, and 0.05% P 20. Both buffers were adjusted to pH 7.4 at room temperature. In experiments with the low-molecular-weight inhibitors, 1% DMSO was included. Buffer B was sterile-filtered through a 0.22  $\mu$ m Millipore filter (Millipore Corp., Bedford, MA) and degassed by sonication for 3 min.

**Computer Modeling.** The models of active PAI-1 were generated in Sybyl (Tripos, St. Louis, MO).

**Expression and Preparation of the PAI-1 Mutants.** All mutants were constructed by site-directed mutagenesis (21), purified from the medium of CHO cells, and activated, applying the same method used for the purification and activation of wt-PAI-1 (19). In one case (C3-PAI-1), the mutation had changed the isoelectric point to such a degree that it was necessary to change the pH in the ion-exchange chromatography correspondingly. Cleaved L2-PAI-1 was prepared by incubating L2-PAI-1 with catalytic amounts of tPA (1/20) for 1 h in assay buffer.

**Determination of the Stability and Specific Activity of the PAI-1 Mutants.** Wt-PAI-1 purified from the medium of CHO cells has lost activity and needs therefore to be activated. The latent form of the PAI-1 variants has therefore been reactivated by the denaturant guanidine-HCl (19). The specific activity is defined as the fraction of total PAI-1 that, after the activation procedure, is able to form an irreversible complex with tPA. The specific activity was determined by titration with an assay in which the remaining tPA activity after preincubation with different amounts of PAI-1 was determined with the chromogenic substrate Flavigen, as previously described (20, 22). Alternatively, the PAI-1 activity was determined by SDS-PAGE (19) after preincubation of 7  $\mu$ M PAI-1 with a slight molar excess (1.3-fold)

of tPA in buffer A for 15 min at 37 °C. SDS-PAGE was performed on PhastGel Gradient 8–25 gels with a Phast-System electrophoresis unit, and the evaluation of the stained gels was performed with an ImageMaster, all obtained from Pharmacia Biotech AB (Uppsala, Sweden). The stability of PAI-1 was determined as the functional half-lives,  $T_{1/2}$ . The different PAI-1 variants were incubated for different periods of time at 25 or 37 °C in 0.1 M sodium acetate buffer at pH 5.5 before determination of the specific activity with tPA in the chromogenic assay; see above.

**Chromogenic Assay for Inhibitors of PAI-1.** Flavigen was used to monitor tPA activity at 405 nm and to quantify PAI-1 activity and inhibition, as described previously (16). The assay was performed at 25 °C in buffer A containing 0.5 mM Flavigen and 1% DMSO under second-order conditions of 4 nM tPA and 3 nM active PAI-1, either wt or mutant, in the presence or absence of AR-H029953XX.  $IC_{50}$  values were estimated from the concentration of AR-H029953XX needed to reduce the absorbance difference after 10 min between the assay in the absence and presence of PAI-1 to 50%. As a control, the highest concentration of AR-H029953XX was also used in the absence of PAI-1 to rule out interference with other components in the assay. In the same type of assay with 4 nM tPA, but with 50  $\mu$ M Flavigen, substrate competition between the chromogenic substrate and 100 nM L2-PAI-1 was measured and the effect of AR-H029953XX studied.

**Characterization of Substrate Behavior of the PAI-1 Mutants.** The different PAI-1 variants (6  $\mu$ M) were incubated at 25 °C in buffer A for 1 h with either a slight molar excess (7.5  $\mu$ M) or catalytic amounts (0.3  $\mu$ M) of tPA. Analysis was made by SDS-PAGE from the appearance of a band with a molecular weight slightly lower than that of wt-PAI-1, corresponding to the molecular weight of cleaved PAI-1 (23).

**Surface Plasmon Resonance.** A BIAcore 2000 analytical system from BIAcore AB, equipped with the analytical software for evaluation of the kinetics (BIAevaluation 2.1), was used. Proteins were immobilized via primary amine groups to the dextran surface of the BIAcore CM5 sensor chip, as described previously (16, 20). Surface densities of immobilized proteins were chosen on the basis of the desired requirement. When antibodies were immobilized on the sensor surface, 100 mM HCl was used for regeneration, allowing the surface to be used for multiple, reproducible experiments. All BIAcore analyses were performed at 25 °C and at a flow rate of 5  $\mu$ L/min. The theory for the evaluation of the kinetic constants has previously been published (16). When more than two components were used in the system, the dissociation between the molecules not involved in the interaction to be measured was shown to be several orders of magnitude lower than the measured dissociation. By simulation of the kinetic experiments using the BIASimulation software, mass transport was shown to be of no importance in these experiments. In contrast, the experiments used to determine the concentrations of non-inhibited PAI-1 were carried out under conditions of semi-mass transport (24).

**Characterization of the Substrate Behavior of L2-PAI-1.** A large density of wt-PAI-1 and L2-PAI-1 (17 kRU) was immobilized on different sensor chip surfaces. Then, 30 nM tPA was injected over both surfaces for 10 min, and the

association and dissociation phases were followed. In a parallel control experiment, tPA was injected over a surface that was activated and deactivated in the absence of PAI-1.

**Binding of PAI-1 to tPA.** The different PAI-1 mutants (10 nM active protein) were injected over a low density of tPA (300 RU), bound on the antibody B10 (500 RU) on immobilized RAM Fc (11 kRU), and the association and dissociation phases were followed. As a control, the same concentration of the mutants was injected over the surface in the absence of tPA. The effect of AR-H029953XX on the binding of PAI-1 to tPA was monitored using tPA captured (800 RU) on the antibody B10 (1.1 kRU), bound on immobilized RAMFc (12 kRU). The rate of binding of 10 nM active wt-PAI-1 in the presence of different concentrations of AR-H029953XX was used to determine the  $IC_{50}$  value. Then, the rate of binding of the PAI-1 variants (10 nM active protein) to tPA in the presence and absence of 25  $\mu$ M AR-H029953XX was used to investigate the effect of the different mutations. As a control, AR-H029953XX was also injected in the absence of PAI-1 to rule out interference with tPA, the antibodies, or the sensor surface.

**Binding of PAI-1 to CLB-2C8.** Different PAI-1 mutants (30 nM) were injected over a low density of CLB-2C8 (300 RU), captured on immobilized RAM Fc (2.3 kRU), and the association and dissociation phases were followed. As a control, the same concentration of the mutants was injected over the surface in the absence of CLB-2C8. Binding of C3-PAI-1 and wt-PAI-1 was compared and further characterized in a matched control experiment by injecting various concentrations (2–10 nM) of these two proteins over an identical amount of captured CLB-2C8 on the same RAM Fc surface. The effect of AR-H029953XX on the binding of PAI-1 to CLB-2C8 was monitored using a high density of CLB-2C8 captured (1.2 kRU) on immobilized RAM Fc (12 kRU). The rate of binding of wt-PAI-1 and the different PAI-1 mutants (10 nM total protein) to CLB-2C8, in the presence of 25  $\mu$ M AR-H029953XX, was used to investigate the effect of the different mutations. As a control, AR-H029953XX was also injected in the absence of PAI-1 to rule out interference with the antibodies or the sensor surface.

## RESULTS

**General Characterization of the Mutants.** The loop mutations were predicted to prevent insertion of strand 4A into  $\beta$ -sheet A and thereby confer substrate behavior and conformational stability to PAI-1. However, the mutant L1-PAI-1 (P10, Ser337Glu) had the inhibitory properties of wt-PAI-1. After activation, a specific activity of L1-PAI-1 of 70% was obtained. The stability of L1-PAI-1 at pH 5.5 was similar to that of wt-PAI-1. In acetate buffer at pH 5.5, wt-PAI-1 had a  $T_{1/2}$  of 88 h at 25 °C and 20 h at 37 °C. In contrast, L2-PAI-1 (P12, Ala335Glu) behaved as a substrate for tPA. As shown by SDS-PAGE (see Figure 4), catalytic amounts of tPA (1/20) completely cleaved L2-PAI-1 after incubation in buffer A at room temperature for 1 h, confirming its substrate behavior. L2-PAI-1 was completely stable as a substrate form in buffer at pH 5.5 and room temperature for several months, as confirmed by SDS-PAGE (not shown).

The second class of mutants were all found to have stability and activity similar to those of wt-PAI-1. C1-PAI-1

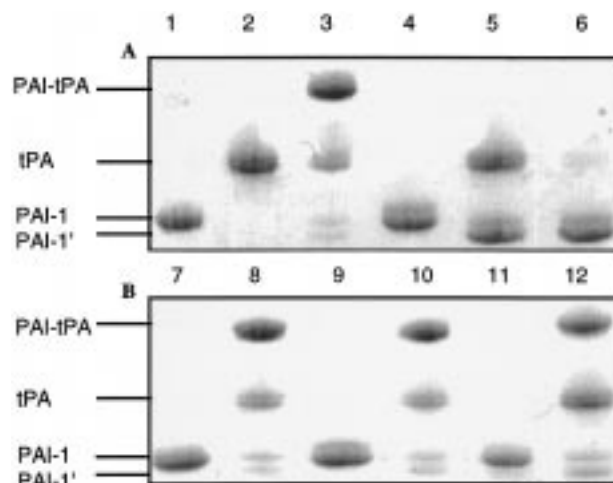


**FIGURE 4:** Densitogram of PAI-1 mutants incubated with tPA. Different PAI-1 mutants (6  $\mu$ M) incubated in buffer A at 25 °C for 1 h in the presence or absence of tPA (7.5  $\mu$ M). Proteins were separated by SDS-PAGE (8–25 gradient) under nonreducing conditions and stained with Coomassie Brilliant Blue. Gel A: lane 1, wt-PAI-1; lane 2, tPA; lane 3, wt-PAI-1 and tPA; lane 4, L2-PAI-1; lane 5, L2-PAI-1 and tPA; and lane 6, L2-PAI-1 and catalytic amounts of tPA (0.3  $\mu$ M). Gel B: lane 7, C1-PAI-1; lane 8, C1-PAI-1 and tPA; lane 9, C2-PAI-1; lane 10, C2-PAI-1 and tPA; lane 11, C3-PAI-1; and lane 12, C3-PAI-1 and tPA. The arrows indicate the direction of migration. PAI-1 (47 kDa), cleaved PAI-1, PAI-1' (43 kDa), tPA (65 kDa), and the PAI-tPA complex (112 kDa).

(Phe114Glu) was activated to a specific activity of 70%; C2-PAI-1 (Val121Phe) and C3-PAI-1 (Arg76Glu/Arg115Glu/Arg118Glu) were activated to a specific activity of 50%, and C4-PAI-1 (Arg115Glu) was activated to a specific activity of 85%. The deviation in the specific activity of the various mutants was within the range found for different batches of wt-PAI-1 (22). As shown in Figure 4, SDS-PAGE of the mutants in this class showed trace amounts of cleaved PAI-1 in the presence of tPA (lanes 8, 10, and 12) similar to that formed with wt-PAI-1 (lane 3).

**Substrate Properties of L2-PAI-1.** As shown in Figure 4, only the mutant L2-PAI-1 was completely cleaved by tPA and there was no trace of an SDS-stable complex between tPA and L2-PAI-1. The binding course of tPA to captured wt-PAI-1 monitored by the BIAcore instrument is characterized by a very rapid association phase and the formation of a stoichiometric stable complex, as has previously been shown (20). In contrast, with a large density of immobilized L2-PAI-1, no stable complex was formed, since after association tPA rapidly dissociated again (Figure 5).

**Inhibition of PAI-1 Analyzed in the Chromogenic Assay and by SDS-PAGE.** The inhibitory effect of AR-H029953XX under second-order conditions of PAI-1 and tPA with the chromogenic tPA substrate was quantified by the apparent  $IC_{50}$  values. Since this substrate decreased the half-life of PAI-1 (20), these  $IC_{50}$  values are slightly underestimated, compared to the values obtained by the BIAcore experiments. SDS-PAGE demonstrated that incubation of PAI-1 with 100  $\mu$ M AR-H029953XX before addition of an excess of tPA did not increase the relative amount of cleaved PAI-1 (not shown). The inhibitor AR-H029953XX thus did not convert PAI-1 into a substrate for tPA. In the chromogenic assay, the progress phase for inhibition of tPA was similar for the same concentration of L1-, C1-, C2-, C3-, and C4-PAI-1 as

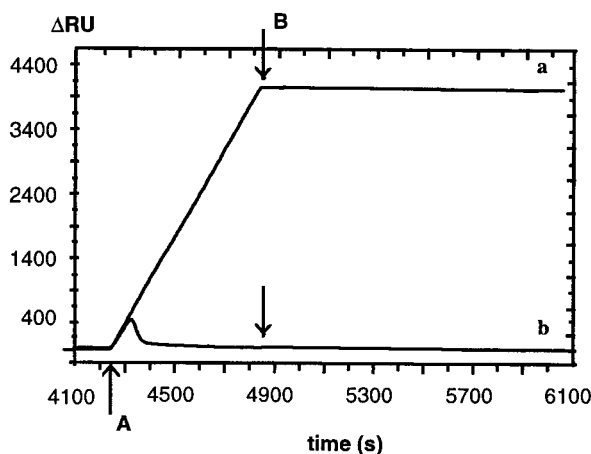


FIGURE 5: Affinity of tPA for immobilized PAI-1. BIAcore 2000 binding and dissociation in buffer B at 5  $\mu\text{L}/\text{min}$  and 25  $^{\circ}\text{C}$ . At arrow A, 30 nM tPA was injected over the surface of amine-coupled PAI-1 (17 kRU), either wt-PAI-1 (a) or L2-PAI-1 (b). At arrow B, the flow was changed to buffer B.

that with wt-PAI-1 (not shown), indicating the same association rate constant for complex formation. Although similar  $\text{IC}_{50}$  values for AR-H029953XX (12  $\mu\text{M}$ ) were found with L1-, C1-, C2-, and C4-PAI-1 and with wt-PAI-1, no inhibition of C3-PAI-1 was found; see Figure 6. Within this class of low-molecular-weight compounds, the acidic function is essential for inhibitory activity. For example, full activity was retained in the tetrazole analogue, whereas the corresponding amidino or nitro derivatives were found to be 2 orders of magnitude less potent. The original substance *N*-[3-(trifluoromethyl)phenyl]anthranilic acid had an  $\text{IC}_{50}$  value of 100  $\mu\text{M}$  in this assay. The absence of an effect of AR-H029953XX with C3-PAI-1 suggests a lack of binding of this class of compounds to C3-PAI-1. Furthermore, substrate competition by L2-PAI-1 in this assay was also inhibited by AR-H029953XX, since in the presence of AR-H029953XX less inhibition of 50  $\mu\text{M}$  Flavin hydrolysis by 100 nM L2-PAI-1 was found (not shown). Accordingly, mutations in the reactive center loop at P10 or P12 did not prevent an inhibitory effect of AR-H029953XX.

**Binding of PAI-1 to tPA Using the BIAcore Instrument.** The binding rate to a low density of captured tPA by the same concentration of active PAI-1 or wt-PAI-1, L1-, C1-, C2-, C3-, or C4-PAI-1 was similar, suggesting the same association rate constant as found before for wt-PAI-1 (16). Furthermore, consistent with the results in the chromogenic assay, AR-H029953XX inhibited the binding rate of active PAI-1 to a large density of tPA, with an apparent  $K_i$  ( $\text{IC}_{50}$ ) of 25  $\mu\text{M}$ ; see Figure 7. Comparison of the effect of AR-H029953XX on different mutants under identical conditions showed that this compound at 25  $\mu\text{M}$  seems to have an effect on L1-, C1-, and C2-PAI-1 similar to that found for wt-PAI-1. In contrast, but in accordance with the results of the chromogenic assay, the binding of C3-PAI-1 to tPA was almost unaffected by this compound, again suggesting that the binding site for the compound is disturbed in this mutant.

**Binding of PAI-1 to CLB-2C8 Using the BIAcore Instrument.** Similar binding rates were found to a small density of the captured monoclonal antibody CLB-2C8 with the same concentrations of L1-, L2-, C1-, C2-, and C4-PAI-1 as were found with wt-PAI-1. We have shown before that this inhibiting antibody binds to a specific epitope on PAI-1 and

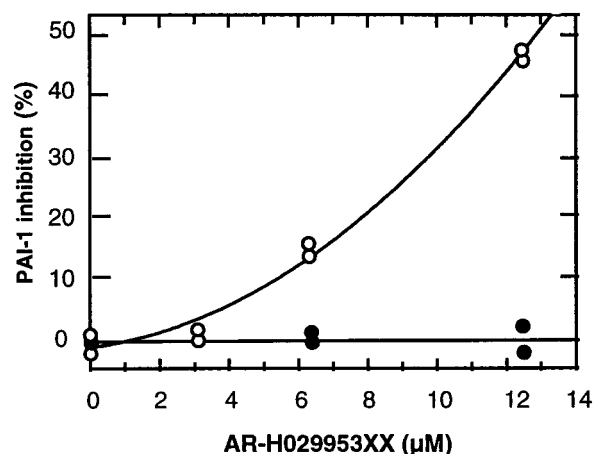


FIGURE 6: PAI-1 inhibition by AR-H029953XX in the chromogenic assay. Absorbance was measured at 405 nm, 10 min after initiation of hydrolysis of 0.5 mM Flavin by 4 nM tPA in buffer A at 25  $^{\circ}\text{C}$ . Values in the absence and presence of 3 nM PAI-1 [wt- (○) or C3-PAI-1 (●)] and AR-H029953XX. PAI-1 inhibition (%), defined as the part of the absorbance shift given by PAI-1 that AR-H029953XX is able to restore, is plotted vs the concentration of added AR-H029953XX.

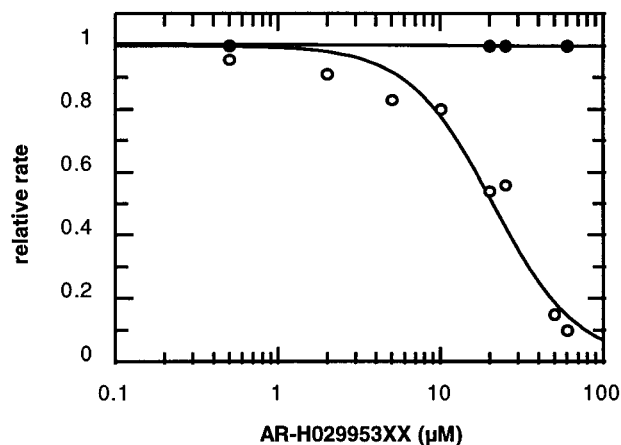


FIGURE 7: Dose titration of the effect of AR-H029953XX on the rate of binding of PAI-1 to tPA using the BIAcore instrument. The binding rate,  $\text{dRU}/\text{dt}$ , of 10 nM active wt-PAI-1 (○) or C3-PAI-1 (●) to tPA (450 RU), captured on B10 (1.1 kRU) on immobilized RAM Fc (12 kRU), in the presence of different concentrations of AR-H029953XX. The flow was 5  $\mu\text{L}/\text{min}$  in buffer B at 25  $^{\circ}\text{C}$ .

has the same high affinity for both the latent and the active form of PAI-1 (16). In contrast, C3-PAI-1 did bind more slowly to captured CLB-2C8 than did wt-PAI-1. Further analysis of the rate constants in a matched control experiment on the same antibody surface (see Figure 8), showed an effect on both the  $k_a$  and the  $k_d$ , resulting in an increase in the  $K_D$  from 0.26 nM for binding of wt-PAI-1 to 1.3 nM for binding of C3-PAI-1 to CLB-2C8. The inhibition by 25  $\mu\text{M}$  AR-H029953XX of the binding rate of wt-PAI-1, L1-, L2-, C1-, C2-, or C4-PAI-1 to CLB-2C8 was similar. Like the observed lack of effect by AR-H029953XX on complex formation of C3-PAI-1 with tPA, this compound did not inhibit the binding of that mutant to CLB-2C8. Mutations in this site thus hinder binding of this compound. Furthermore, in contrast to wt-PAI-1, 25  $\mu\text{M}$  AR-H029953XX could not decrease the rate of binding of either cleaved L2-PAI-1 or latent wt-PAI-1 to CLB-2C8.

The results in the three different assays with the low-molecular-weight inhibitor AR-H029953XX and the different

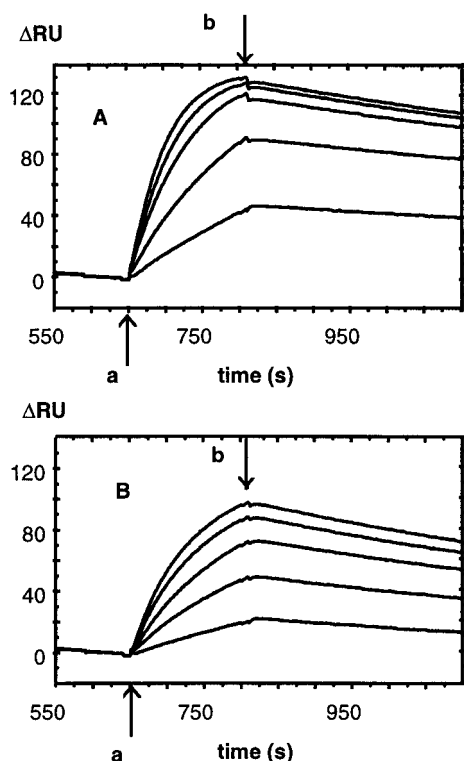


FIGURE 8: Binding kinetics, measured by the BIAcore instrument, of the binding of PAI-1 to captured CLB-2C8 (300 RU) on immobilized RAM Fc (2.3 kRU). At arrow a, different concentrations of PAI-1 (2–10 nM total protein) were injected, and at arrow b, the protein was replaced by buffer. The flow was 5 mL/min in buffer B at 25 °C. Values are given  $\pm$  standard deviation for the curve fitting. (A) wt-PAI-1,  $k_a = (2.4 \pm 0.09) \times 10^6 \text{ M}^{-1} \text{ s}^{-1}$ ,  $k_d = (0.63 \pm 0.09) \times 10^{-3} \text{ s}^{-1}$ , and  $K_D = 0.26 \text{ nM}$ . (B) C3-PAI-1,  $k_a = (1.4 \pm 0.04) \times 10^6 \text{ M}^{-1} \text{ s}^{-1}$ ,  $k_d = (1.7 \pm 0.02) \times 10^{-3} \text{ s}^{-1}$ , and  $K_D = 1.3 \text{ nM}$ .

PAI-1 variants are listed in Table 1. In conclusion, only C3-PAI-1 was in all assays found to be insensitive to the presence of AR-H029953XX.

## DISCUSSION

In latent PAI-1, 13 residues of the reactive center loop (P16–P4) are inserted into  $\beta$ -sheet A as strand 4A (10). This “insertion” site, between strands 3A and 5A, is an obvious epitope for a serpin inhibitor, as has also been proven for antithrombin (25, 26),  $\alpha_1$ -antitrypsin (27), and PAI-1 (6, 7) using different segments of the loop structure. However, in contrast to the effect of these peptides, AR-H029953XX did not induce cleavage of PAI-1 by tPA. This compound thus did not convert PAI-1 into a substrate for tPA. Moreover, the modifications of the residues P10 and P12 in our two loop mutants, L1- and L2-PAI-1, did not prevent inhibition by the low-molecular-weight inhibitor AR-H029953XX. The inhibition mechanism of this compound may therefore not be directly related to loop insertion.

Consistent with our mutant L2-PAI-1 with a charged Glu residue at P12, the PAI-1 variant in which the Ala at position P12 was substituted with Pro (12) created stable substrate PAI-1. However, in the study by Tucker et al. in which unglycosylated PAI-1 produced in *Escherichia coli* was used (14), the replacement of Ala at P12 with Glu did not convert the serpin into a substrate for tPA. This unexpected difference may thus be due to the presence or absence of

Table 1: Effect of 25  $\mu\text{M}$  AR-H029953XX on PAI-1 Mutants<sup>a</sup> in Different Assays<sup>c</sup>

assay	active wt	latent wt	L1	L2	cleaved L2	C1	C2	C3	C4
chromogenic assay <sup>b</sup>	+	nb	+	+	nb	+	+	–	+
binding to tPA <sup>c</sup>	+	nb	+	nd	nb	+	+	–	nd
binding to CLB-2C8 <sup>d</sup>	+	–	+	+	–	+	+	–	+

<sup>a</sup> L1-PAI-1 (Ser337Glu), L2-PAI-1 (Ala335Glu), C1-PAI-1 (Phe114Glu), C2-PAI-1 (Val121Phe), C3-PAI-1 (Arg76Glu/Arg115Glu/Arg118Glu), and C4-PAI-1 (Arg115Glu). <sup>b</sup> To monitor the progress phase of inhibition of tPA activity, 3 nM active PAI-1 and 0.5 mM Flavigen with and without AR-H029953XX in buffer A were mixed with 4 nM tPA at 25 °C and the  $\Delta A$  at 405 nm was measured over the course of 10 min. With L2-PAI-1, 50  $\mu\text{M}$  Flavigen and 100 nM total PAI-1 were used instead. <sup>c</sup> The rate of binding of 10 nM active PAI-1 in the absence or presence of AR-H029953XX to tPA (0.8 kRU) bound to B10 (1.1 kRU), captured on amine-coupled RAM Fc (12 kRU), was measured by the BIAcore instrument. The flow rate was 5  $\mu\text{L}/\text{min}$  in buffer B at 25 °C. <sup>d</sup> The binding rate of 10 nM PAI-1 (total protein) in the absence or presence of AR-H029953XX to CLB-2C8 (1.2 kRU) captured on amine-coupled RAM Fc (12 kRU) was measured by the BIAcore instrument. The flow rate was 5  $\mu\text{L}/\text{min}$  in buffer B at 25 °C. <sup>e</sup> + = inhibition by AR-H029953XX. – = no or minor effect of AR-H029953XX. nb = no binding by PAI-1 could be measured in the absence of AR-H029953XX. nd = not determined.

glycosylation. In the structure of PAI-1, three potential glycosylation sites are present, of which we can exclude interference of glycans linked to Asn209 and Asn265, since these are located on the “backside” of PAI-1. Instead, the third potential site, Asn329 in strand 5A of  $\beta$ -sheet A, may bind a glycan responsible for sterical or charge effects at the insertion side. In disagreement with the conclusion by Tucker et al. (14), we suggest therefore that insertion of P12 may be required for inhibitory activity of PAI-1. This conclusion is also drawn for two other serpins, antithrombin and C1-inhibitor (9, 25, 26). Our P10 Glu mutant, L1-PAI-1, was not a substrate for tPA, in contrast with the study in which the P10 Ser337 was substituted with Pro (12). Since in the structure of latent PAI-1 there is no space for a large substituent like Glu, this suggests that P10 cannot be inserted. This difference between two amino acids in this position again emphasizes the role of insertion in the reaction mechanism of serpins (28).

The binding site for the very potent inhibiting antibody CLB-2C8 has been demonstrated by our antibody study to be one of three epitopes on PAI-1 involved in the formation of the stable complex with tPA (16). The location of the binding epitope for CLB-2C8 was first determined to be on a linear peptide containing the residues 110–145 (17), which later was restricted to residues 128–145 (18). Within the area of this postulated epitope, we found a hydrophobic cleft, near residues Phe114 and Val121, flanked by a basic surface region containing three arginine residues (76, 115, and 118). Docking experiments with AR-H029953XX suggested that this new domain might constitute a binding site for the low-molecular-weight inhibitor, and we decided to seek evidence for this hypothesis by altering the hydrophobic cleft as well as the charged region by using site-directed mutagenesis. Other parts of this region which have been said to be involved in the pathway to the final complex with tPA, as for example helix F (29), are completely exposed to the

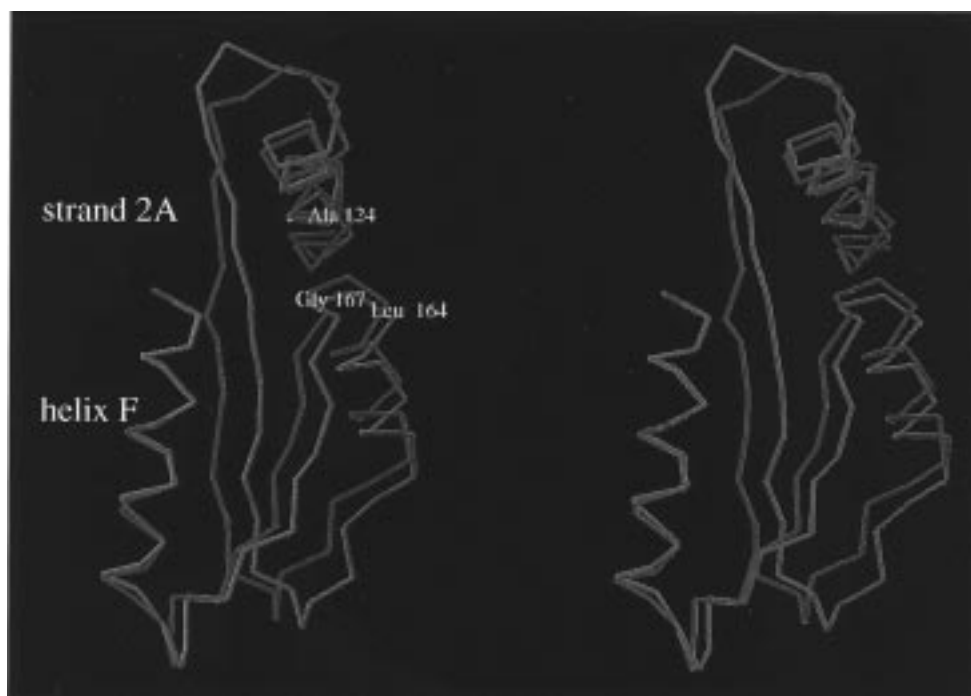


FIGURE 9: Stereoview of the area in antithrombin (30) corresponding to the area around the epitope for CLB-2C8 in active and latent PAI-1. Helix F of both active (green) and latent (magenta) antithrombin were superimposed. The indicated residues Ala124, Gly167, and Leu164 correspond to Arg76, Arg110, and Arg115 in PAI-1, respectively.

solvent and do not contain attractive binding sites for small inhibitors. As shown in Figures 2 and 3, the mutated residues in C3-PAI-1 (76, 115, and 118) are still located close to the folded peptide sequence 128–145. Therefore, the different binding affinities of CLB-2C8 for C3-PAI-1 and for wt-PAI-1 might be consistent with either of the two previously suggested epitopes for CLB-2C8. The unambiguous diminished effect of AR-H029953XX on C3-PAI-1, compared to that on wt-PAI-1, further confirmed the involvement of this area in the reaction between PAI-1 and tPA. Inspection of possible modes of binding of AR-H029953XX to PAI-1 within the region of the binding epitope for CLB-2C8 reveals two plausible sites of interaction: a salt bridge between the carboxylate group of AR-H029953XX and one or more of the three arginines (Arg76, Arg115, and Arg118) and a hydrophobic interaction between the dichlorophenyl moiety of AR-H029953XX and a lipophilic assembly of side chains in the vicinity of Val121 and Phe114 (see Figure 3). The importance of the acidic moiety in the compound supports the existence of a salt bridge. Introduction of three negatively charged residues, as in C3-PAI-1, apparently abolishes binding of AR-H029953XX, whereas alteration of the lipophilic area alone, as in C1- and C2-PAI-1, seems to be tolerated by AR-H029953XX. This loss of effect on C3-PAI-1 also suggests that the binding epitope for both CLB-2C8 and AR-H029953XX is close to either Arg76, Arg115, Arg118, or all of them. Since C4-PAI-1 still can be inhibited by AR-H029953XX, the involvement of Arg115 in these two binding-sites and in the complex formation between PAI-1 and tPA can of course be questioned, but it is possible that alteration of this residue alone is not enough for discrimination. Finally, inspection of the model structure of the protein could not reveal any conformational changes when these mutations were introduced.

Although AR-H029953XX has the same inhibitory effect on the binding of uncleaved L2-PAI-1 and of wt-PAI-1 to

CLB-2C8, our results show the lack of an effect of AR-H029953XX not only on cleaved L2-PAI-1 but also on latent PAI-1. This suggests an additional conformational difference in this region near the CLB-2C8 epitope of PAI-1 after insertion of the reactive center loop. Comparison of the same area in the corresponding structure for latent and active antithrombin (30) did reveal some differences. As can be seen in Figure 9, the fact that the reaction center loop is inserted as a new strand in  $\beta$ -sheet A of latent antithrombin has moved this specific area out from the molecule in the latent conformation, compared to that in active antithrombin. It may well be that this difference between the active and the latent conformation also exists in PAI-1. This assumption is also strengthened by our finding that AR-H029953XX discriminates between latent and cleaved PAI-1 on one hand and active and uncleaved substrate PAI-1 on the other hand. One must, however, keep in mind that Figure 3 depicts the site as found in latent PAI-1 (10) and therefore cannot represent the precise position of the involved residues in active PAI-1. Preliminary results have also shown that another serpin,  $\alpha_2$ -antiplasmin, was not inhibited by AR-H029953XX, indicating that the correct conformation of this site is important for interaction with this low-molecular-weight inhibitor.

The involvement of this secondary binding site in the interaction of PAI-1 with tPA is of special interest. The strongly inhibiting antibody CLB-2C8 binds to PAI-1 in complex with tPA with the same affinity as it does with active and latent PAI-1 (16). The position of tPA in the final complex with PAI-1 can thereby not overlap the binding site for this antibody. The position of this site (see Figure 2) is opposite the reactive center loop where the bait region for attack of the protease is. In the model proposed by Wright and Scarsdale (31), this area of the serpin can be imagined to be involved in the pathway to the final stable complex. In another recent publication, using fluorescent

probes on both sides of the P1–P1' cleavage site, the conclusion was drawn that tPA in the final complex with PAI-1 has instead migrated to a position on the surface of  $\beta$ -sheet A (29). Altogether, the final position of serine proteinases in the irreversible complex with serpins still has to be proven in detail. This new region is, however, an attractive site for inhibition of PAI-1 activity, and is undoubtedly affected during complex formation between tPA and this serpin. Further studies are needed to reveal the inhibition mechanism of AR-H029953XX.

In conclusion, the fact that AR-H029953XX did not inhibit the binding of C3-PAI-1 to either tPA or the antibody CLB-2C8, as is the case with wt-PAI-1, strongly suggests that the binding epitope for this type of PAI-1 inhibitor is close to Arg76 and/or Arg118. Moreover, since AR-H029953XX no longer inhibited the binding of latent PAI-1, or of cleaved PAI-1 to CLB-2C8, the actual conformation at this site in active PAI-1 must be different from the conformation in latent and cleaved PAI-1.

## ACKNOWLEDGMENT

We are grateful to Åsa Emanuelsson and Anna-Karin Nilsson for the genetic constructions, to Thord Johansson for cell culturing, and to Christer Westerlund, Mark Harris, Mats Kihlén, and Derek Ogg for their valuable suggestions during the design of the different PAI-1 mutants. We are also indebted to Robin Carrell and Richard Skinner for making available to us the coordinates of antithrombin, to Paul Declerck for the coordinates of cleaved PAI-1, and to Elizabeth Goldsmith for the coordinates of latent PAI-1.

## REFERENCES

1. van Meijer, M., and Pannekoek, H. (1995) *Fibrinolysis* 9, 263–276.
2. Hamsten, A., and Eriksson, P. (1992) *Fibrinolysis* 8, 253–262.
3. Biemond, B. J., Levi, M., Coronel, R., Jansen, M. J., ten Cate, J. W., and Pannekoek, H. (1995) *Circulation* 91, 1175–1181.
4. Abrahamsson, T., Nerme, V., Strömquist, B., Åkerblom, B., Legnèd, A., Pettersson, K., and Westin-Eriksson, A. (1996) *Thromb. Haemostasis* 75, 118–126.
5. Charlton, P. A., Faint, R. W., Bent, F., Folkes, A., Templeton, D., Mackie, I., Machin, S., and Bevan, P. (1997) *Fibrinolysis Proteolysis* 11, 51–56.
6. Eitzman, D. T., Fay, W. P., Lawrence, D. A., Francis-Chmura, A. M., Shore, J. D., Olson, S. T., and Ginsburg, D. (1995) *J. Clin. Invest.* 95, 2416–2420.
7. Kvassman, J. O., Lawrence, D. A., and Shore, J. D. (1995) *J. Biol. Chem.* 270, 27942–27947.
8. Von Kaulla, K. N., and von Kaulla, E. (1978) in *Progress in chemical fibrinolysis and thrombolysis*, Vol. 3, pp 451–459, Raven Press, New York.
9. Carrell, R. W., Stein, P. E., Fermi, G., and Wardell, M. R. (1994) *Structure* 2, 257–270.
10. Mottonen, J., Strand, A., Symersky, J., Sweet, R. M., Danley, D. E., Geoghegan, K. F., Gerard, R. D., and Goldsmith, E. J. (1992) *Nature* 355, 270–273.
11. Aertgeerts, K., De Bondt, H. L., and De Ranter, C. (1995) *J. Struct. Biol.* 113, 239–245.
12. Audenaert, A., Knockaert, I., Collen, D., and Declerck, P. J. (1994) *J. Biol. Chem.* 269, 19559–19564.
13. Lawrence, D. A., Olson, S. T., Palaniappan, S., and Ginsburg, D. (1994) *J. Biol. Chem.* 269, 27657–27662.
14. Tucker, H. M., Mottonen, J., Goldsmith, E. J., and Gerard, R. D. (1995) *Nat. Struct. Biol.* 2, 442–445.
15. Berkenpas, M. B., Lawrence, D. A., and Ginsburg, D. (1995) *EMBO J.* 14, 2969–2977.
16. Björquist, P., Ehnebom, J., Inghardt, T., and Deinum, J. (1997) *Biochim. Biophys. Acta* 1341, 87–98.
17. Keijer, J., Linders, M., van Zonneveld, A.-J., Ehrlich, H. J., de Boer, J.-P., and Pannekoek, H. (1991) *Blood* 78, 401–409.
18. van Zonneveld, A.-J., van den Berg, B. M., van Meijer, M., and Pannekoek, H. (1995) *Gene* 167, 49–52.
19. Strömquist, M., Andersson, J.-O., Boström, S., Deinum, J., Ehnebom, J., Enquist, K., Johansson, T., and Hansson, L. (1994) *Protein Expression Purif.* 5, 309–316.
20. Björquist, P., Brohlin, M., Ehnebom, J., Ericsson, M., Kristiansen, C., Pohl, G., and Deinum, J. (1994) *Biochim. Biophys. Acta* 1209, 191–202.
21. Hansson, L., Blackberg, L., Edlund, M., Lundberg, L., Strömquist, M., and Hermell, O. (1993) *J. Biol. Chem.* 268, 26692–26698.
22. Ehnebom, J., Björquist, P., Andersson, J.-O., Johansson, T., and Deinum, J. (1997) *Fibrinolysis Proteolysis* 11, 165–170.
23. Strömquist, M., Karlsson, K.-E., Björquist, P., Andersson, J.-O., Byström, M., Hansson, L., Johansson, T., and Deinum, J. (1996) *Biochim. Biophys. Acta* 1295, 103–109.
24. Christensson, L. L. H. (1997) *Anal. Biochem.* 249, 153–164.
25. Björk, I., Ylinenjärvi, K., Olson, S. T., and Bock, P. E. (1992) *J. Biol. Chem.* 267, 1976–1982.
26. Björk, I., Nordling, K., and Olson, S. T. (1993) *Biochemistry* 32, 6501–6505.
27. Schultze, A. J., Baumann, U., Knof, S., Jaeger, E., Huber, R., and Laurell, C. B. (1990) *Eur. J. Biochem.* 194, 51–56.
28. Gettins, P. G. W., Patson, P. A., and Olson, S. T. (1996) in *Serpins: Structure, Function and Biology*, Springer-Verlag, Heidelberg.
29. Wilczynska, M., Fa, M., Karolin, J., Ohlsson, P.-I., Johansson, L. B.-Å., and Ny, T. (1997) *Nat. Struct. Biol.* 4, 354–357.
30. Skinner, R., Abrahams, J.-P., Whisstock, J. C., Lesk, A. M., Carrell, R., and Wardell, M. R. (1997) *J. Mol. Biol.* 266, 601–609.
31. Wright, H. T., and Scarsdale, J. N. (1995) *Proteins* 22, 210–225.

BI971554Q